R-502 AND TWO NEAR-AZEOTROPIC ALTERNATIVES
PART I: INTUBE FLOW BOILING TESTS

N. Kattan is a Ph.D. candidate, Department of Mechanical Engineering, Swiss Federal Institute of Technology, Lausanne, Switzerland; **J.R. Thome** is Visiting Professor, Department of Mechanical Engineering, Swiss Federal Institute of Technology, Lausanne, Switzerland; **D. Favrat** is Professor, Department of Mechanical Engineering, Swiss Federal Institute of Technology, Lausanne, Switzerland.

N. Kattan, J.R. Thome (Ph.D.) and D. Favrat (Ph.D., ASHRAE Member)

ABSTRACT

Intube flow boiling experiments for two new non-azeotropic, three-component refrigerant mixtures (HP80 and HP62) and R-502, the azeotropic refrigerant binary mixture they are replacing, have been carried out. Comparative results show that local flow boiling heat transfer coefficients for HP62 are slightly larger than those for R-502 under the same test conditions while those for HP80 are on average slightly smaller. The heat transfer performances of the three fluids are accurately predicted by an existing flow boiling correlation modified here to include a nucleate boiling mixture correlation.

KEY WORDS: Azeotrope, Boiling, Evaporation, Heat Transfer, Refrigerant Mixtures

---

[Submitted to ASHRAE Meeting, Orlando, FL, June 25-29, 1994].

R-502 AND TWO NEAR-AZEOTROPIC ALTERNATIVES
PART I: INTUBE FLOW BOILING TESTS

ABSTRACT

Intube flow boiling experiments for two new non-azeotropic, three-component refrigerant mixtures (HP80 and HP62) and R-502, the azeotropic refrigerant binary mixture they are replacing, have been carried out. Comparative results show that local flow boiling heat transfer coefficients for HP62 are slightly larger than those for R-502 under the same test conditions while those for HP80 are on average slightly smaller. The heat transfer performances of the three fluids are accurately predicted by an existing flow boiling correlation modified here to include a nucleate boiling mixture correlation.

INTRODUCTION

A two-phase flow and heat transfer test program was undertaken to obtain flow boiling test data for two new replacements for R-502 and secondly to compare their thermal performances to that of R-502. The two new refrigerants tested were:

HP80 (60% R-125/2% R-290/38% R-22, by wt.) known as R-402A

and

HP62 (44% R-125/52% R-143a/4% R-134a, by wt.) known as R-404A

The present paper focuses on intube boiling heat transfer while a companion paper [Kattan, Thome and Favrat (1994)] covers two-phase flow patterns for the same tests.

Flow boiling of non-azeotropic refrigerant mixtures has recently become an important research topic while work on other mixture systems, principally binary and multi-component hydrocarbon mixtures and aqueous mixtures has already been underway for several decades. Many fundamental results for

these latter mixtures are analytically-based and can be applied to refrigerant mixtures. For a comprehensive review of forced convective boiling of pure fluids and mixtures, the reader is referred to Collier and Thome (1994). For a complete review of mixture boiling fundamentals, refer to Thome and Shock (1984). For a survey of enhanced boiling of mixtures, see Thome (1990).

TEST FACILITIES, EQUIPMENT AND PROCEDURES

The experimental work was conducted using the test facility at the Laboratoire d'Energétique Industrielle at the Ecole Polytechnique Fédérale de Lausanne. Two-phase experiments to measure heat transfer coefficients and pressure drops and record flow patterns can be run simultaneously. Flows can be investigated in horizontal, vertical or inclined orientations. The present tests were run with <u>horizontal</u> test sections.

Figure 1 depicts a simplified flow diagram of the test facility. It has four double-pipe test sections (only two are shown). One pair of double-pipe sections mounted in series is used with the test fluid (i.e. refrigerant) flowing inside the inner tube [configuration for the present tests] and the another pair can be used with the test fluid flowing in the annulus. Heat is supplied via hot water flowing counter-currently to the test fluid; it can be directed to either pair of test sections.

As shown in Figure 1, the test fluid passes through an electrical preheater before reaching the first test section. After passing through the two test sections the test fluid enters a coiled tube-in-tube condenser. Next it is drawn into a stainless steel pump with a magnetically driven rotor, the latter which operates without any lubricating oil and eliminates any

possibility of oil from entering the test fluid loop. A speed control on the pump is used to modify the flow rate of the test fluid. The subcooled test fluid then passes through a calibrated Coriolis flow meter and back into the preheaters. A temperature-controlled receiver is connected via a valve to the test fluid circuit to regulate the amount of refrigerant charge and a high vacuum pump system (not shown) is also connected for evacuation and for leak detection tests. A sample bottle was also connected into the test fluid circuit.

The chilled water-glycol solution circulated through the condenser is cooled with a separate R-502 refrigeration system. The water-glycol flow loop includes a large liquid receiver, a setup which eliminates cyclical temperature variations in the test fluid's coiled tube-in-tube condenser that could otherwise arise from the on-off operating characteristics of the R-502 refrigeration system.

The hot water flow rate is measured by a calibrated, high quality float meter. The hot water is circulated by a stainless steel pump similar to the refrigerant circuit's to eliminate corrosion and/or rust formation and to prevent any possibility of lubricating oil entering the water circuit and thus affecting the energy balances. This system is carefully deaerated to eliminate any adverse effects on heat transfer, flow rate measurements and energy balances.

A data acquisition system together with a PC computer are used to acquire, analyze and store the data. The thermocouples are calibrated using the double precision method available in the acquisition system to obtain the highest accuracies possible, that is 0.05°F (0.03°C). For adiabatic conditions after leaving

the rig off all night, all temperatures are within a maximum deviation of 0.18°F (0.10°C) and most are within 0.09°F (0.05°C) of the average.

For diabatic test conditions, the maximum variations between the four thermocouple readings around the annuli at any one position are normally within 0.18°F (0.10°C) or less [about 0.05°F (0.03°C)] for the hot water when its Re_D > 3000. The uniformity of these temperature measurements also confirms the precision centering of the copper tube. The temperature variations are larger (0.36-0.54°F, 0.20-0.30°C) for Re_D < 3000, where thermal stratification becomes significant in the hot water due to the natural convection effects of mixed convection. All the present tests were thus run with water-side Re_D > 3200. In addition, the minimum temperature decrease for the hot water across any test zone was set at 0.54°F (0.30°C) for the data to be considered of acceptable accuracy. To substantiate this cutoff, data obtained for water temperature drops from 0.54-0.72°F (0.30-0.40°C) were found to compare well with those with larger temperature drops at similar test conditions.

The refrigerant flow rate is measured with an estimated accuracy of 0.2% and the water flow rate to within 1.0%, based on our calibrations. The energy balances between the water and refrigerant flows in the two test sections agree to within 2% maximum error (1% average error) when the hot water's Reynolds number is maintained above 3000, which is within the accuracy of published specific heat values for refrigerants and water. Errors can rise to 3-5% for Re_D < 3000 because of the thermal stratification effect and hence this test regime is avoided.

Repeatability of experimental data is very good. It is

estimated that heat transfer coefficients are measured within a maximum error of about 7.5% but usually less, depending on the test conditions.

TEST SECTIONS

The outer tubes of the double-pipe test sections are a novel design; they are precision machined in two halves from PVC Hard, which is a very hard and durable plastic material that also insulates the test section. This allows the dimensions to be very precise and uniform along the length, much more than the standard piping normally used. An O-ring is compressed between the two halves to form the seal such that the two halves meet to form a circular annulus around the inner copper tube. The internal diameter of the PVC pipe is 0.787 in. (20.00 mm). O-ring sealed screws are inserted through the outer PVC tube to center the copper tube inside and the PVC tube is supported too.

Figure 2 shows the test section measurement layout diagram for hot water flowing in the annulus and refrigerant flowing counter-currently inside the inner tube. At the refrigerant inlet, the temperature is measured by thermocouple #600 located in the refrigerant flow stream (the tube is well insulated from this point up to the location of the four water-side thermocouples #614, #613, #501 and #615 with a tightly-fitted teflon sleeve). Similar arrangements exist for the measured refrigerant temperatures #601, #602 and #603, respectively. At each of these locations the absolute pressures of the refrigerant and the differential pressure drops across the two test sections are measured. In addition, tubular sight glass sections of 12.00 mm bore are installed inline with the tube to visualize the flow near these four locations.

On the water-side, four thermocouples are installed at each measurement location in the annulus at 0°, 60°, 120° and 180° from the top of the annulus. These are inserted through sealed screws installed in the thick outer PVC tube wall with the junctions positioned about 0.04 in. (1 mm) from the copper tube wall. There are four measurement locations on both the top and bottom test sections; thus, there are six test zones to obtain heat transfer coefficients over narrow changes of vapor quality (essentially local values) during boiling tests. This approach eliminates inlet, outlet and "dead" zones formed at the connections to the mixing chambers used in conventional setups that significantly alter the local water-side heat transfer coefficients over a sizable portion of the test section length. Using the present setup, a minimum of flow disruption of the hot water flow results and the highly accurate energy balances confirm the integrity of this approach.

The test sections (inner tubes of the double-pipes) are plain, drawn copper tubing. They had internal diameters of 0.472 inch (12.00 mm) and outside diameters of 0.551 inch (14.00 mm). Each of the two test sections is 9.89 ft. (3.013 m) long for heat transfer measurements; each test section is divided into 3 test zones as shown in Figure 2. The external diameters of the copper tubes were also measured to be uniform along their length.

The six test zones allow six heat transfer coefficients to be determined simultaneously over successive narrow changes in vapor quality in each zone. These coefficients are mean values for each zone but are essentially local heat transfer coefficients because of the small change in quality (on the order of 3-8%) from inlet to outlet of each zone. Consequently, the tests

provide heat transfer data as a function of vapor quality similar to those obtained in electrically-heated test sections. Test facilities with one long test section provide only mean values over a wide change in vapor quality that may include both wet wall and dry-out regions. Because stratified flow can exist in horizontal tubes, electrically-heated test sections are not appropriate since the unwetted wall then acts as a fin and a very non-uniform heat flux distribution around the circumference of the tube occurs. Hot water heating instead provides essentially a uniform wall temperature around the tube similar to actual operating equipment.

MODIFIED WILSON PLOTS

Traditional modified Wilson plot methods are based on the Dittus-Boelter type of turbulent flow heat transfer correlation. However, this can yield large scatter in the heating water data because this correlation cannot model the transition flow regime, i.e. $2300 < Re_D < 10{,}000$, a common range for the hot water in refrigerant boiling tests. A new approach was thus developed based instead on the Gnielinski (1976) heat transfer correlation applicable for the range $2300 < Re_D < 1{,}000{,}000$. Using this approach, single-phase turbulent flow data obtained for R-134a flowing inside the test section tube agree with the Gnieliski correlation predictions within 5% or less. The water-side heat transfer coefficients in the double-pipes ranged from 572 to 704 Btu/h $ft^2 \cdot F$ (3250 to 4000 W/m^2 K).

TEST FLUIDS

HP80 and HP62 are three-component, "near-azeotropic" mixtures. The boiling ranges (dew point temperature minus bubble point

temperature) of HP80 and HP62 are 1.8°F and 0.8°F (1.01°C and 0.45°C), respectively. R-502 is a binary azeotropic mixture composed of 48.8% R-22/51.2% R-115 and thus its boiling range is zero.

The tests were run at fixed saturation temperatures and mass velocities such that direct comparison of experimental heat transfer data for the three fluids could be made at similar heat fluxes over a wide range of local vapor qualities. Table 1 depicts the range of the test variables. The saturation temperatures for the near-azeotropic mixtures are their bubble point temperatures, which correspond to the inlet condition at the entrance to the first heated test section.

The physical properties of the three fluids are compared in Table 2 at 36.3°F (2.4°C). The thermodynamic and transport properties of R-502 were predicted from standard ASHRAE methods. The thermodynamic properties for HP80 and HP62 were obtained from tables provided by the manufacturer (Du Pont) and their transport properties were predicted using REFPROP (1992). Since REFPROP did not accurately predict the vapor pressure curves of HP80 and HP62 using its own internal binary interaction parameters, these parameters were input and good agreement was then obtained.

Handling of multi-component mixtures must be done carefully in order to ensure that the composition of the sample does not change during its introduction into the test facility nor during the experimental tests themselves. For example, as liquid is withdrawn from a closed vessel, part of the liquid remaining behind must evaporate in order to fill the volume orginally occupied by this liquid. Since the vapor compositions are not the same as those in the liquid phase for a non-azeotropic

mixture, the liquid composition changes during this process. This effect is particularly acute for mixtures with large differences in vapor and liquid compositions, but are minor for near-azeotropics such as HP80 and HP62.

In order to double-check the present handling procedures, small liquid samples were obtained for the following fluids: (i) the original HP80 as supplied by the manufacturer, (ii) the liquid within the test circuit midway through the HP80 tests, and (iii) the liquid in the test circuit at the conclusion of the HP80 tests. Two composition measurements of each of these three samples were then measured by the manufacturer. Table 3 shows the results. The average value of each sample tested was within the normal product range for HP80. Two minor unidentified components make up about 0.5% of the fluid. A small increment of 0.7% in R-125 composition was registered from the beginning to the end of the tests. [Samples were also taken for HP62 but have not yet been analyzed].

DEFINITION OF MIXTURE BOILING HEAT TRANSFER COEFFICIENTS

The heat transfer coefficient for boiling in a pure fluid is defined with the wall temperature T_w and the saturation temperature T_{sat} as

$$\alpha = q/(T_w - T_{sat}) \tag{1}$$

For a mixture, the heat transfer coefficient is defined using the bubble point temperature corresponding to the local bulk liquid concentration at the local saturation pressure. Thus

$$\alpha = q/(T_w - T_{bub}) \tag{2}$$

Examining Eq. (2), it is seen that T_{bub} becomes equal to T_{sat} for the two pure components, and the definition is consistent.

During the evaporation of a non-azeotropic mixture, the vapor composition of the more volatile component (lower boiling point fluid) is larger than its composition in the liquid phase. Consequently, the local bubble point temperature increases as the composition of the less volatile component (higher boiling point fluid) in the liquid phase rises during evaporation along a heated tube. The change in enthalpy H of the mixture during evaporation along the tube is thus comprised of three terms:

$$dH = h_{LV}\, dx + (1-x)\, dT_{bub}\, (c_p)_L + x\, dT_{bub}\, (c_p)_V \qquad (3)$$

These are (i) the latent heat of vaporization of the amount vaporized dx, (ii) the sensible heating of the liquid phase (1-x) and (iii) the sensible heating of the vapor phase x. The values of h_{LV}, $(c_p)_L$ and $(c_p)_V$ are a function of the local liquid and vapor compositions. In calculating the local heat transfer coefficients along the tube, Eq. (2) must be used together with phase equilibria data to determine the local vapor quality, local heat flux and T_{bub}. Equation (3) reduces to only the latent heat for a pure fluid or an azeotrope as expected.

For boiling, the enthalpy or heat release curve given by Eq. (3) is known as the evaporation curve and a unique curve exists at each saturation pressure. For consistency, this curve is used to reduce test data to boiling heat transfer coefficients and should also be utilized for designing multi-component evaporators to calculate local temperatures and enthalpy changes. For HP80 and HP62 the heat release curves were determined using REFPROP with user-supplied binary interaction parameters. These curves were then fit to produce expressions for local vapor quality and bubble point temperature as a function of enthalpy as follows:

$$x = a_1\, (H+H_o)^2 + a_2\, (H+H_o) + a_3 \qquad (4)$$

and

$$T_{bub} = b_1 (H+H_o)^3 + b_2 (H+H_o)^2 + b_3 (H+H_o) + b_4 \quad (5)$$

The values of the constants for HP80 and HP62 at the three test conditions are given in Table 4. H_o is the reference enthalpy at a vapor quality of 0.0 and H is the enthalpy relative to H_o.

The inlet condition at the first test zone for the refrigerant was 0.5°F (0.3°C) of subcooling. Then, using the heat duty lost by the hot water in the first test zone, the vapor quality and bubble point temperature at the exit of the zone were calculated using Eqs. (4) and (5). In this manner, the local conditions at the end of the other zones were determined in successive steps. Using the mean bubble point temperature for the zone, Eq. (2) was then used to calculate the boiling heat transfer coefficient for the zone utilizing the water-side coefficient, the heat duty and the log mean temperature difference (LMTD) for the zone and taking into account the wall resistance of the copper tube.

PREDICTION OF FLOW BOILING HEAT TRANSFER TO MIXTURES

There are many correlations for flow boiling of pure fluids inside horizontal tubes and several methods have also been proposed for non-azeotropic refrigerant mixtures. For a recent review, see Collier and Thome (1994). None of the correlations for non-azeotropic mixtures has yet been shown to apply to a data set other than the original one used for its development. Also these methods ignore the effect of heat flux on the mixture boiling correction term.

The present tests were compared to the two correlations of Gungor and Winterton (1986, 1987). The contribution of nucleate boiling in these two correlations was corrected for mixture effects utilizing the Thome (1989) nucleate pool boiling

equation, which gives the mixture effect as

$$F_c = [1 + (\alpha_I/q)\ \Delta T_{bp}\ [1 - \exp\ (\frac{-\ B_o\ q}{\rho_L\ h_{LV}\ \beta_L})]]^{-1} \qquad (6)$$

where α_I is the ideal heat transfer coefficient calculated with the Gungor-Winterton correlation without mixture effects but with the mixture physical properties, ΔT_{bp} is the boiling range, B_o is a scaling factor assumed to be 1.0 (i.e. the theory assumes all heat transfer at a bubble interface is latent heat), q is the local heat flux attributable to nucleate boiling, ρ_L is the liquid density of the mixture, h_{LV} is the latent heat of the mixture and β_L is the liquid phase mass transfer coefficient that can be assumed to have a constant value of 0.0003 m/s.

Equation (6) is an analytically derived expression and hence should be universally applicable. In fact, the expression has been shown to work for a very wide variety of mixtures, including aqueous mixtures, hydrocarbon mixtures, cryogenic mixtures and refrigerant mixtures. It is accurate up to boiling ranges of 54°F (30°C), above which it provides conservative results. Importantly, the Thome equation includes the effect of heat flux in the mixture correction factor, such that F_c varies from 1.0 at very low heat fluxes up to the boiling range at large heat fluxes. Equation (6) can be incorporated into just about any pure fluid flow boiling correlation.

The Gungor-Winterton (1987) correlation is thus modified to the following expression:

$$\alpha = E\ \alpha_L \qquad (7)$$

where E now includes the mixture correction factor applied to the Boiling number (which models the nucleate boiling contribution to the flow boiling process) such that

$$E = 1 + 3000\ (Bo\ F_c)^{0.86} + 1.12\ [x/(1-x)]^{0.75}\ (\rho_L/\rho_V)^{0.41} \quad (8)$$

For HP80 and HP62, the boiling ranges are very small such that the mixture correction factor F_c is from 0.98 to 0.99, i.e. almost no adverse effect. The rest of the correlation remains the same as before where

$$\alpha_L = 0.023\ [G\ (1-x)\ D_i/\mu_L]^{0.8}\ Pr_L^{0.4}\ (\lambda_L/D_i) \quad (9)$$

$$Bo = q/(G\ h_{LV}) \quad (10)$$

For liquid Froude numbers less than 0.05, an additional correction for stratified flow is applied to E, such that

$$\alpha = E\alpha_L\ Fr_L^{(0.1\ -\ 2\ Fr_L)} \quad (11)$$

where

$$Fr_L = G^2/[\rho_L^2\ D_i\ g] \quad (12)$$

The Gungor-Winterton (1987) correlation combines the nucleate boiling and convective contributions to heat transfer together in one term, i.e. Eq. (8). Therefore, the heat flux attributable to nucleate boiling cannot be determined to obtain q for use in Eq. (6). Consequently, the total heat flux has been used for q.

The Gungor-Winterton (1986) correlation is similarly modified such that

$$\alpha = E_o\alpha_L + S\alpha_{pool}\ F_c \quad (13)$$

F_c and α_L are the same as described above and F_c modifies the nucleate boiling contribution to heat transfer. For the definitions of E_o, S and α_{pool}, refer to their paper. Because boiling suppression factor S multiplies the nucleate pool boiling coefficient and S is also a function of E_o, it is not possible to isolate the heat flux attributable to nucleate boiling without resorting to an iterative solution; thus it is reasonable to use the total heat flux for q in Eq. (6).

EXPERIMENTAL RESULTS

Not all the test results can be presented here because of space limitations. In tests using hot water as a heating source it is not possible to run tests at pre-established heat fluxes since the heat flux depends on many system parameters. Thus, the data presented are grouped into ranges of heat flux, such as 2536-3171 Btu/h ft^2 (8000-10000 W/m^2). Since the coefficients are functions of heat flux, it should be noted that part of the scatter of the data points shown on the following graphs is due to this variation in q for different data points shown. In any case, this type of presentation allows trends in the data to be illustrated.

Figure 3(a) depicts the boiling data for HP80 at mass velocities of 73515, 147030 and 233778 lb/h ft^2 (100, 200 and 318 kg/m^2 s) for the heat flux range of 2536-3171 Btu/h ft^2 (8000-10000 W/m^2), a bubble point temperature of 36.3°F (2.4°C) and a pressure of 102.2 psia (7.05 bar). Figure 3(b) depicts the boiling data for HP62 at mass velocities of 73515, 147030 and 233778 lb/h ft^2 (100, 200 and 318 kg/m^2 s) for the heat flux range of 2536-3171 Btu/h ft^2 (8000-10000 W/m^2), a bubble point temperature of 36.3°F (2.4°C) and a pressure of 95.8 psia (6.605 bar). Figure 3(c) depicts the boiling data for R-502 at mass velocities of 73515, 147030 and 220545 lb/h ft^2 (100, 200 and 300 kg/m^2 s) for the heat flux range of 2536-3171 Btu/h ft^2 (8000-10000 W/m^2), a bubble point temperature of 36.5°F (2.5°C) and a pressure of 89.8 psia (6.19 bar).

In Figures 3(a), 3(b) and 3(c) a distinct maximum in heat transfer coefficient at a vapor quality of about 8% is observed at the highest mass velocity while a more moderate one occurs at

about 15% at the medium mass velocity. The heat transfer coefficient is seen to decrease monotonically with increasing vapor quality at the lowest mass flow rate. The maxima may be caused by a change in flow pattern or other physical processes, such as the onset of nucleate boiling, and is being investigated further. A moderate increase in the heat transfer coefficient is observed with mass velocity as expected.

The effect of heat flux is shown in Figure 4(a) for the boiling data of HP80 at a mass velocity of 74985 lb/h ft^2 (102 kg/m^2 s), a bubble point temperature of 36.3°F (2.4°C) and a pressure of 102.2 psia (7.05 bar). The three heat flux ranges are 1427-1807, 2536-3171 and 4534-5327 Btu/h ft^2 (4500-5700, 8200-10400 and 14300-16800 W/m^2). A significant increase in the heat transfer coefficient with heat flux is observed as expected. The heat transfer coefficients trail off to lower values at high vapor qualities.

The heat flux effect on boiling of HP62 at a mass velocity of 74985 lb/h ft^2 (102 kg/m^2 s), a bubble point temperature of 36.3°F (2.4°C) and a pressure of 95.8 psia (6.605 bar) is depicted in Figure 4(b). The three heat flux ranges are 1585-1902, 1902-2536 and 2536-3171 Btu/h ft^2 (5000-6000, 6000-8000 and 8000-10000 W/m^2). An increase in the heat transfer coefficient with heat flux is again observed and the coefficients trail off to lower values at high vapor qualities.

The effect of saturation pressure (and dew point temperature) on heat transfer is shown in Figure 5(a) for HP80 at a heat flux range of 4439-5390 Btu/h ft^2 (14000-17000 W/m^2). The pressures represented are 91.2, 102.2 and 128.6 psia (6.29, 7.05 and 8.87 bar). The corresponding dew point temperatures are 29.7, 36.3

and 50.4°F (-1.3, 2.4 and 10.2°C). A small increase in the coefficients with rising pressure is found. Figure 5(b) illustrates a similar effect of saturation pressure on heat transfer for HP62 for the heat flux range of 4439-5390 Btu/h ft^2 (14000-17000 W/m^2). The pressures represented are 85.4, 95.7 and 121.2 psia (5.89, 6.60 and 8.36 bar). The corresponding dew point temperatures are 29.7, 36.3 and 50.4°F (-1.3, 2.4 and 10.2°C). A small increase in the coefficients with rising pressure is again evident.

COMPARISON OF HP80 AND HP62 TO R-502 AND CORRELATIONS

Design heat fluxes in actual evaporators normally range from about 1902 to 3171 Btu/h ft^2 (6000-10000 W/m^2) when utilizing plain copper tubes. The comparisons below are therefore made in this heat flux range over a wide variation in local vapor quality.

Figure 6 depicts a direct comparison of experimental boiling coefficients of HP80 and HP62 to R-502 at a fixed inlet dew point temperature of 36.3-36.7°F (2.4-2.6°C) and also shows their confrontation with the Gungor and Winterton (1986, 1987) correlations [GW86 and GW87, respectively]. The test conditions are for a mass velocity of 73151 lb/h ft^2 (100 kg/m^2 s) and a heat flux range of 1902-2536 Btu/h ft^2 (6000-8000 W/m^2).

Figure 6(a) illustrates that the heat transfer coefficients are very similar over the vapor quality range from 10-90%. HP80 tends to have a thermal performance slightly below that of R-502 while that of HP62 is almost the same. Figure 6(b) depicts a comparison of the two correlations to the HP80 data. The Gungor-Winterton (1987) correlation including the Thome mixture boiling correction factor F_c accurately predicts this data. The Gungor-

Winterton (1986) correlation including F_c grossly overpredicts this data. Figure 6(c) shows similar results for HP62. Instead, Figure 6(d) shows that both correlations predict the R-502 data accurately. The average coefficients for the data in Figure 6(a) are 217, 244 and 249 (1229, 1384 and 1413 W/m^2 K) for HP80, HP62 and R-502, respectively; the values for HP80 and HP62 are -13% and -2% relative to that of R-502, respectively.

Figure 7 depicts a similar comparison for the heat flux range of 2536-3171 Btu/h ft^2 (8000-10000 W/m^2). Figure 7(a) illustrates that the heat transfer coefficients are very similar over the vapor quality range from 10-88%. HP80 again tends to have a thermal performance slightly below that of R-502 while HP62 is slightly better. In Figure 7(b) the Gungor-Winterton (1987) correlation including F_c underpredicts the HP80 data while the 1986 correlation including F_c still significantly overpredicts this data. Figure 7(c) for HP62 shows the same trends as HP80. Instead, Figure 7(d) shows that both correlations tend to underpredict this R-502 data. The average coefficients for the data in Figure 7(a) are 270, 311 and 300 (1531, 1767 and 1703 W/m^2 K) for HP80, HP62 and R-502, respectively; the values for HP80 and HP62 are -10% and +4% relative to that of R-502, respectively.

Figure 8 depicts the comparison for the heat flux range of 2536-3171 Btu/h ft^2 (8000-10000 W/m^2) at a mass velocity of 147030 lb/h ft^2 (200 kg/m^2 s). Figure 8(a) illustrates that the heat transfer coefficients are very similar over the vapor quality range from 5-52%. Minor maxima in the heat transfer coefficient at a vapor quality of 12-15% are found for all three fluids. In Figure 8(b) the Gungor-Winterton (1987) correlation

including F_c slightly underpredicts the HP80 data while the 1986 correlation including F_c still overpredicts this data. Figure 8(c) for HP62 shows better accuracy is attained by the 1987 correlation, although with the wrong trend relative to vapor quality. The 1986 version again significantly overpredicts all the data. Instead, Figure 8(d) for R-502 gives comparisons similar to those for HP62. The average coefficients for the data in Figure 8(a) are 351, 355 and 327 (1995, 2018 and 1856 W/m^2 K) for HP80, HP62 and R-502, respectively; the values for HP80 and HP62 are +8% and +9% relative to that of R-502, respectively.

Figure 9 shows a comparison for the heat flux range of 2536-3171 Btu/h ft^2 (8000-10000 W/m^2) over a mass velocity of 220545-233778 lb/h ft^2 (300-318 kg/m^2 s). Figure 9(a) again confirms that the heat transfer coefficients of the three refrigerants are very similar, over vapor qualities from 3-29%. More prominent maxima in the heat transfer coefficient are found for all three fluids at this higher mass velocity but the location has shifted to lower vapor qualities of 5-7%. In Figure 9(b) the Gungor-Winterton (1987) correlation including F_c accurately predicts the HP80 data except for the maximum while the 1986 correlation predicts the data in the maximum well and overpredicts the rest of the data. HP62 in Figure 9(c) and R-502 in Figure 9(d) depict the same trends as HP80. The average coefficients for the data in Figure 9(a) are 382, 401 and 387 (2168, 2275 and 2200 W/m^2 K) for HP80, HP62 and R-502, respectively; the values for HP80 and HP62 are -1% and +3% relative to that of R-502, respectively.

Reviewing Figures 6, 7, 8 and 9 it is noted that the Gungor-Winterton (1987) correlation models all three fluids reasonably

well. This correlation responds well to the variations in the heat transfer data with mass velocity, vapor quality and fluid. Instead the Gungor-Winterton (1986) correlation works well only for R-502 at the mass velocity of 75314 lb/h ft^2 (100 kg/m^2 s). At higher mass velocities the 1986 correlation grossly overpredicts the data and thus this correlation apparently does not account for the effect of mass velocity very well.

STATISTICAL COMPARISON OF THE CORRELATIONS TO THE DATA

Table 5 provides a summary of the comparison of all the test data to the two Gungor-Winterton correlations corrected for mixture boiling. The Gungor-Winterton (1987) correlation (GW87) is consistently more accurate than their earlier correlation, i.e. (GW86), for HP80, HP62 and R-502, respectively. For all 1011 data points the standard deviation for GW87 is 21.19% while for GW86 it is 27.77%. Work is continuing in this area and the data will also be compared to other correlations later on.

NON-EQUILIBRIUM MIXTURE EFFECTS

Thermocouple readings in the present experiments showed superheating existed with respect to the local bubble point temperature to occur at the thermocouples at the end of the two test sections, not withstanding local vapor qualities significantly below 100%. These were more pronounced for the two near-azeotropic mixtures than for R-502 and can be attributable to non-equilibrium effects during evaporation of these two mixtures. The thermocouple at the entrance to the second test section showed that the two 90 degree bends between the two test sections mixed the flow and eliminated this superheating at the inlet to the second one, such that the measured temperature

agreed with the predicted bubble point temperature. Thus, the non-equilibrium effect increases along the length of an evaporator tube until a bend is confronted by the flow.

EVAPORATOR DESIGN CONSIDERATIONS

The heat transfer coefficients of HP80 and HP62 are very similar to those of R-502 for the same test conditions. Referring to Table 2, the latent heats are quite close for these three fluids and hence the mass flow rates and heat fluxes required to produce the same level of refrigeration duty will be nearly the same. Two major changes in thermal design methods for evaporators using HP80 and HP62 rather than R-502 are to introduce the evaporation curve into (i) the heat duty calculation of the evaporator and (ii) the calculation of the log-mean-temperature-difference (LMTD) of the unit. If the two-phase pressure drop is large enough to have a significant effect on the local bubble point temperature, then the calculation should interpolate between two evaporation curves, i.e. Eqs. (3-5), developed for the inlet and outlet pressures.

CONCLUSIONS

Comparative results show that local flow boiling heat transfer coefficients for HP62 are slightly larger than those for R-502 under the same test conditions while those for HP80 are on average slightly smaller. The heat transfer performances of the three fluids are accurately predicted by an existing flow boiling correlation modified here to include a nucleate boiling mixture correlation. In any case, the mixture effect on HP62 and HP80 is minimal, reducing heat transfer coefficients by only 1-2%.

ACKNOWLEDGEMENTS

The research was supported by the Swiss Federal Office of Energy (OFEN), Bern. The refrigerants were provided by DuPont de Nemours International S.A. of Geneva.

REFERENCES

Collier, J.G. and Thome, J.R., 1994. Convective Boiling and Condensation, 3rd Edition, Oxford University Press, Oxford.

Gnieliski, V., 1976. New Equations for Heat and Mass Transfer in Turbulent Pipe and Channel Flow, Int. Chem. Eng., Vol. 16, pp. 359-368.

Gungor, K.E. and Winterton, R.H.S., 1986. A General Correlation for Flow Boiling in Tubes and Annuli, Int. J. Heat Mass Transfer, Vol. 29, pp. 351-358.

Gungor, K.E. and Winterton, R.H.S., 1987. Simplified General Correlation for Saturated Flow Boiling and Comparisons of Correlations with Data, Chem. Eng. Res. Des., Vol.65, pp. 148-156.

Kattan, N., Thome, J.R. and Favrat, D. (1994). R-502 and Two Near-Azeotropic Alternatives. Part II: Two-Phase Flow Patterns, ASHRAE Trans.

REFPROP (1992). Thermodynamic Properties of Refrigerants and Refrigerant Mixtures, Version 3.04a, National Institute of Standards and Technology (NIST), Gaithersburg, MD.

Thome, J.R., 1989. Prediction of the Mixture Effect on Boiling in Vertical Thermosyphon Reboilers, Heat Transfer Engineering, Vol. 10, No. 2, pp. 29-38.

Thome, J.R. (1990). Enhanced Boiling Heat Transfer, Hemisphere Publ. Corp., New York.

Thome, J.R. and Shock, R.A.W., 1984. Boiling of Multicomponent Mixtures, in Advances in Heat Transfer, Academic Press, Vol. 16, pp. 59-156.

NOTATION

Bo	Boiling number
B_o	Scaling factor (= 1.0)
$(c_p)_L$	Liquid specific heat (kJ/kg K)
$(c_p)_V$	Vapor specific heat (kJ/kg K)
D_i	Internal tube diameter (m)
E	Two-phase convection multiplier defined in Eq. (8)
E_o	Two-phase convection multiplier used in Eq. (13)
F_c	Mixture correction factor
Fr_L	Liquid Froude number
G	Total mass velocity (kg/m^2 s)
g	Gravitational acceleration (9.81 m/s^2)
H	Enthalpy (kJ/kg)
H_o	Reference enthalpy (kJ/kg)
h_{LV}	Latent heat of vaporization (kJ/kg)
Pr_L	Liquid Prandtl number
q	Heat flux (W/m^2)
S	Boiling suppression factor
ΔT_{bp}	Boiling range of mixture (= $T_{dew}-T_{bub}$) (°C)
T_{bub}	Bubble point temperature (°C)
T_{dew}	Dew point temperature (°C)
T_{sat}	Saturation temperature (°C)
T_w	Wall temperature (°C)
x	Vapor quality
α	Local boiling heat transfer coefficient (W/m^2 K)
α_I	Ideal boiling heat transfer coefficient (W/m^2 K)
α_L	Liquid heat transfer coefficient (W/m^2 K)
α_{pool}	Nucleate pool boiling coefficient (W/m^2 K)
β_L	Liquid mass transfer coefficient (m/s)
λ_L	Liquid thermal conductivity (W/m K)
ρ_L	Liquid density (kg/m^3)
ρ_V	Vapor density (kg/m^3)
μ_L	Liquid dynamic viscosity (Ns/m^2)

Table 1. Flow boiling test conditions.

Fluid	T_{sat} °F (°C)	P_{sat} psia (bar)	Mass Velocity 1000 x lb/h ft^2 (kg/m^2 s)	Heat Flux Btu/h ft^2 (W/m^2)	Vapor Quality (%)
HP80:	29.7 (-1.3)	91.4 (6.30)	233 (317)	1428-6606 (4503-20,836)	1.7-54.7
	36.3 (2.4)	102.2 (7.05)	75, 147, 234 (102, 200, 318)	1391-7260 (4387-22,897)	1.7-90.0
	50.4 (10.2)	128.7 (8.88)	223 (303)	1455-9067 (4588-28,597)	2.8-83.6
HP62:	29.7 (-1.3)	85.4 (5.89)	235 (320)	1688-6905 (5323-21,777)	1.9-54.7
	36.3 (2.4)	95.8 (6.61)	75, 147, 234 (102, 200, 318)	1084-9686 (3418-30,551)	1.7-92.1
	50.4 (10.2)	121.2 (8.36)	221 (300)	1386-9693 (4372-30,573)	1.6-89.3
R-502:	36.5 (2.5)	89.9 (6.20)	73.5, 147, 221 (100, 200, 300)	1350-8789 (4257-27,720)	1.8-98.6

Table 2. Physical properties at 36.3°F (2.4°C).

Property	HP80	HP62	R-502
Saturation Pressure psia (bar)	102.2 (7.05)	95.8 (6.61)	89.4 (616.8)
Liquid Density lb/ft^3 (kg/m^3)	78.5 (1257)	72.7 (1164)	82.0 (1313)
Vapor Density lb/ft^3 (kg/m^3)	2.32 (37.2)	2.05 (32.9)	2.18 (34.9)
Liquid viscosity cp ($mN\ s/m^2$)	0.205 (0.205)	0.181 (0.181)	0.226 (0.226)
Vapor Viscosity cp ($mN\ s/m^2$)	0.0122 (0.0122)	0.0117 (0.0117)	0.0121 (0.0121)
Liquid Specific Heat Btu/lb°F (kJ/kg K)	0.289 (1.211)	0.321 (1.346)	0.283 (1.184)
Vapor Specific Heat Btu/lb°F (kJ/kg K)	0.195 (0.817)	0.224 (0.939)	0.169 (0.708)
Liquid Thermal Cond. Btu/h ft °F (W/m K)	0.037 (0.064)	0.044 (0.076)	0.042 (0.073)
Latent Heat Btu/lb (kJ/kg)	68.7 (159.4)	71.7 (166.3)	62.4 (144.9)
Surface Tension (dyne/cm)	8.75	7.46	9.92
Critical Pressure psia (bar)	599.6 (41.35)	538.7 (37.32)	590.9 (40.75)
Molecular Weight	101.55	97.60	111.63
Dew Point Temperature °F (°C)	38.1 (3.4)	37.1 (2.8)	36.3 (2.4)
Bubble Point Temperature °F (°C)	36.3 (2.4)	36.3 (2.4)	36.3 (2.4)

Table 3. HP80 sample compositions (by weight).

Component	Normal	Initial Sample	Intermediate Sample	Final Sample
R-125	60.0%	61.0/61.0	61.4/61.5	61.7/62.7
Propane	2.0%	1.27/1.27	1.23/1.23	1.32/1.26
R-22	38.0%	37.1/37.2	36.7/36.8	36.4/35.4
Unknown 1		0.24/0.25	0.26/0.26	0.25/0.24
Unknown 2		0.30/0.28	0.28/0.28	0.27/0.28

Table 4. Constants for heat release curves of HP80 and HP62 (units are in SI units, i.e. °C and kJ/kg).

Fluid	P_{sat} (bar)	$a_1 \times 10^{-7}$	$a_2 \times 10^{-3}$	a_3	$b_1 \times 10^{-7}$	$b_2 \times 10^{-5}$	b_3	b_4	H_o kJ/kg
HP80	6.30	-5.16	6.570	-1.313	0.0	-1.680	0.0165	-3.966	203.1
	7.05	-4.86	6.670	-1.363	0.0	-1.246	0.0141	-0.037	207.5
	8.88	0.0	6.515	-1.399	0.0	-1.690	0.0164	7.372	217.1
HP62	5.89	-2.52	6.029	-1.178	0.0	0.925	-0.00228	-1.199	197.1
	6.61	0.0	5.993	-1.209	-0.759	7.412	0.02047	4.117	202.0
	8.36	-2.79	6.410	-1.351	-1.362	12.580	-0.0353	13.37	212.7

Table 5. Comparison of Data to Gungor-Winterton correlations.

Fluid	T_{sat} °F (°C)	G lb/h ft^2 (kg/m^2 s)	q Btu/h ft^2 (W/m^2)	x (%)	Data Points	% Standard Deviation GW86	GW87
HP80:	29.7 (-1.3)	233043 (317)	1428-6606 (4503-20,836)	2-55	67	28.35	21.76
	36.3 (2.4)	75985 (102)	1031-5315 (3253-16,765)	4-90	72	34.35	21.38
	36.3 (2.4)	147030 (200)	1039-7260 (3278-22,897)	2-88	108	46.52	37.65
	36.3 (2.4)	233778 (318)	1082-7032 (3414-22,179)	1-61	94	24.63	19.30
	50.4 (10.2)	222750 (303)	795-9067 (2506-28,597)	3-84	102	25.63	20.93
HP62:	29.7 (-1.3)	235248 (320)	1688-6905 (5323-21,777)	2-55	65	26.37	20.97
	36.3 (2.4)	75985 (102)	1084-3280 (3418-10,345)	4-88	59	26.82	20.00
	36.3 (2.4)	147030 (200)	1421-6691 (4483-21,104)	3-91	82	19.31	13.62
	36.3 (2.4)	233778 (318)	1451-9686 (4577-30,551)	2-77	102	20.24	14.98
	50.4 (10.2)	220545 (300)	1386-9693 (4372-30,573)	2-89	93	19.89	13.95
R-502:	36.7 (2.6)	73515 (100)	1348-3539 (4252-11,161)	7-94	36	23.27	19.41
	36.5 (2.5)	147030 (200)	1379-7355 (4349-23,197)	3-99	49	37.73	29.82
	36.3 (2.4)	220545 (300)	1350-8789 (4257-27,720)	2-80	82	27.64	21.59
Total (Mean Error All Data Points):					1011	27.77	21.19

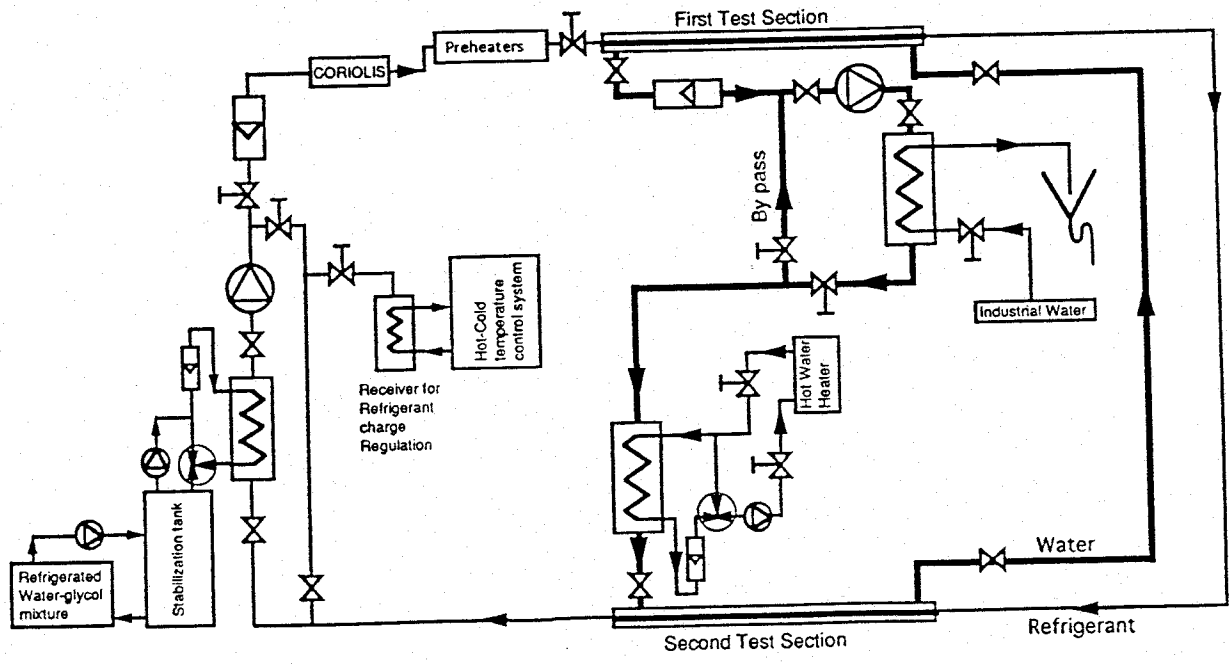

Figure 1. Layout of LENI test facility flow circuits.

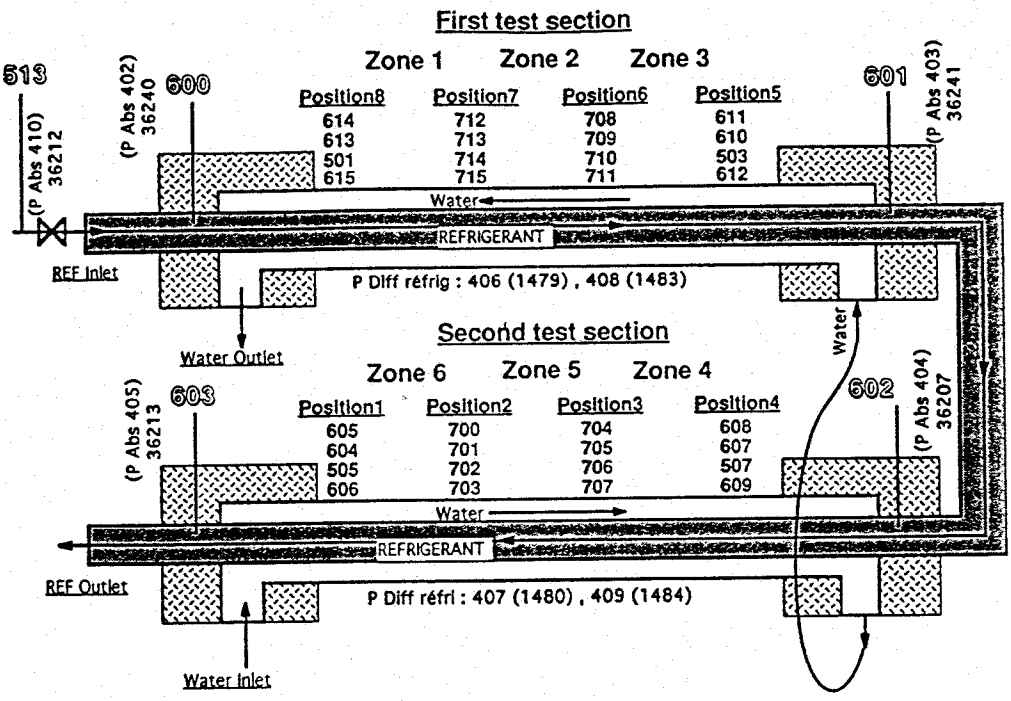

Figure 2. Measurement locations in the test sections.

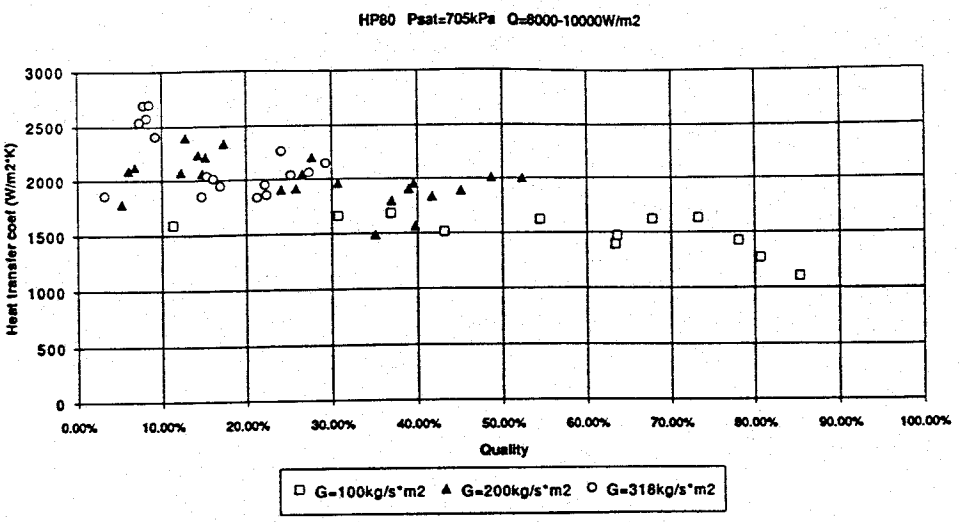

Figure 3(a). HP80 results at three mass velocities.

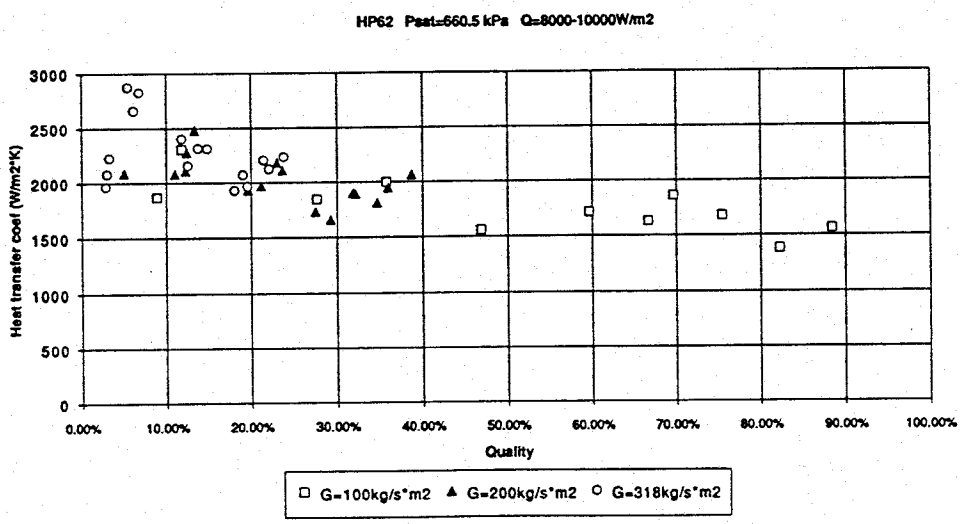

Figure 3(b). HP62 results at three mass velocities.

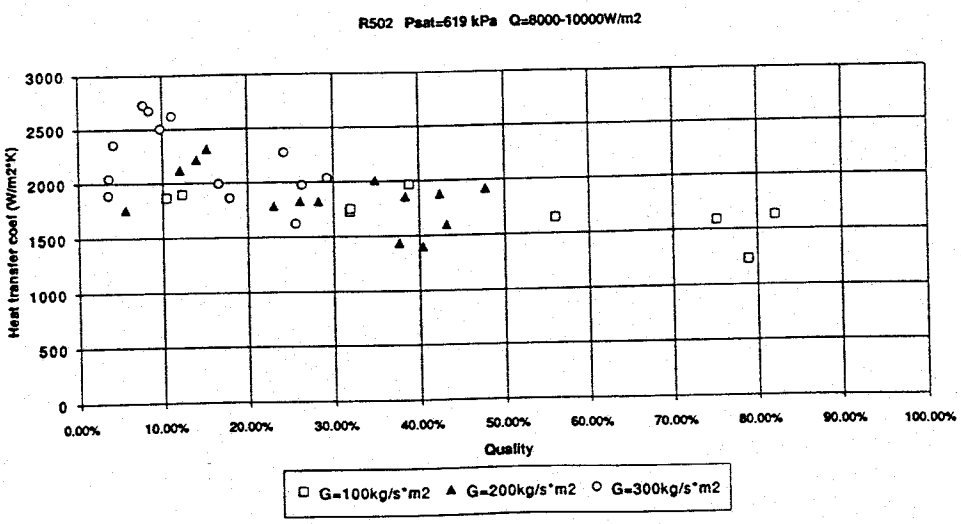

Figure 3(c). R-502 results at three mass velocities.

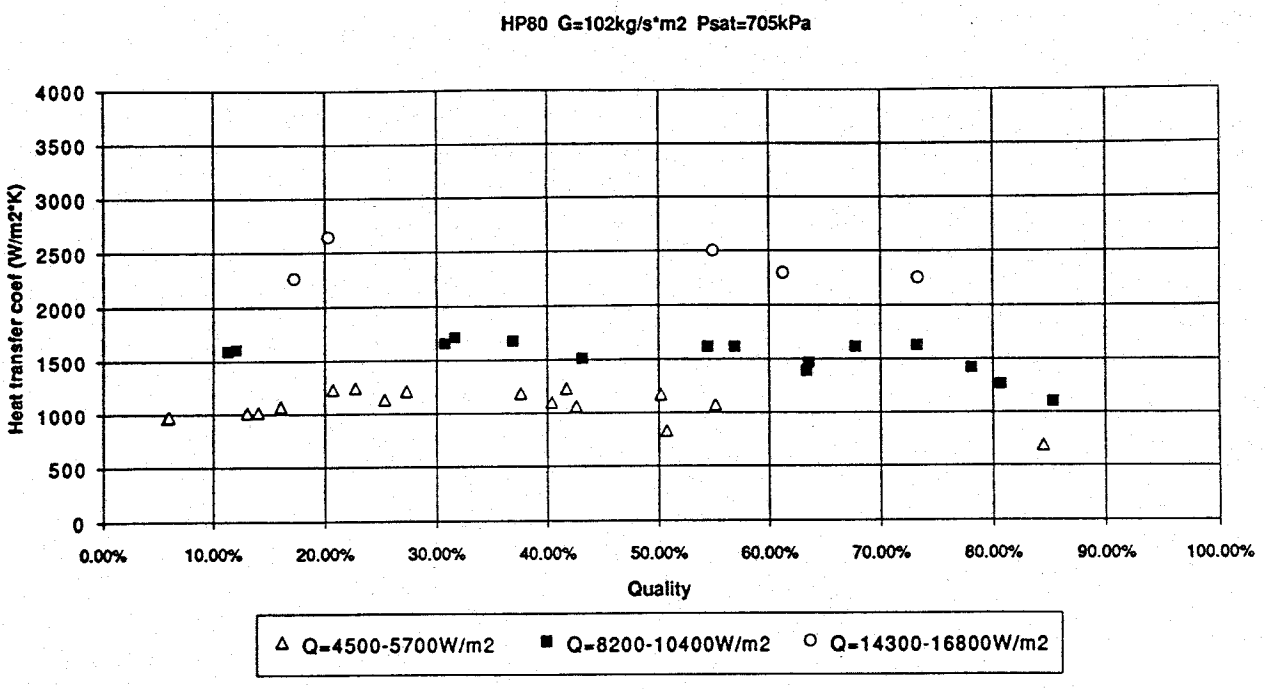

Figure 4(a). HP80 results at three heat fluxes.

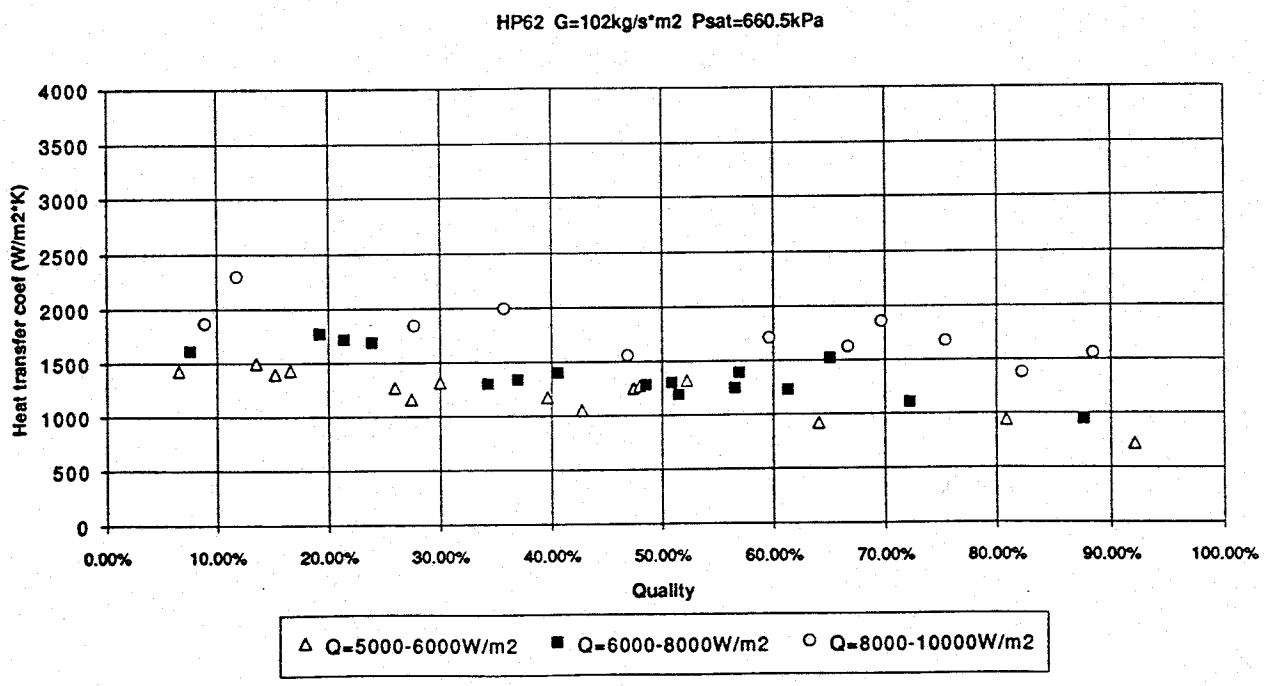

Figure 4(b). HP62 results at three heat fluxes.

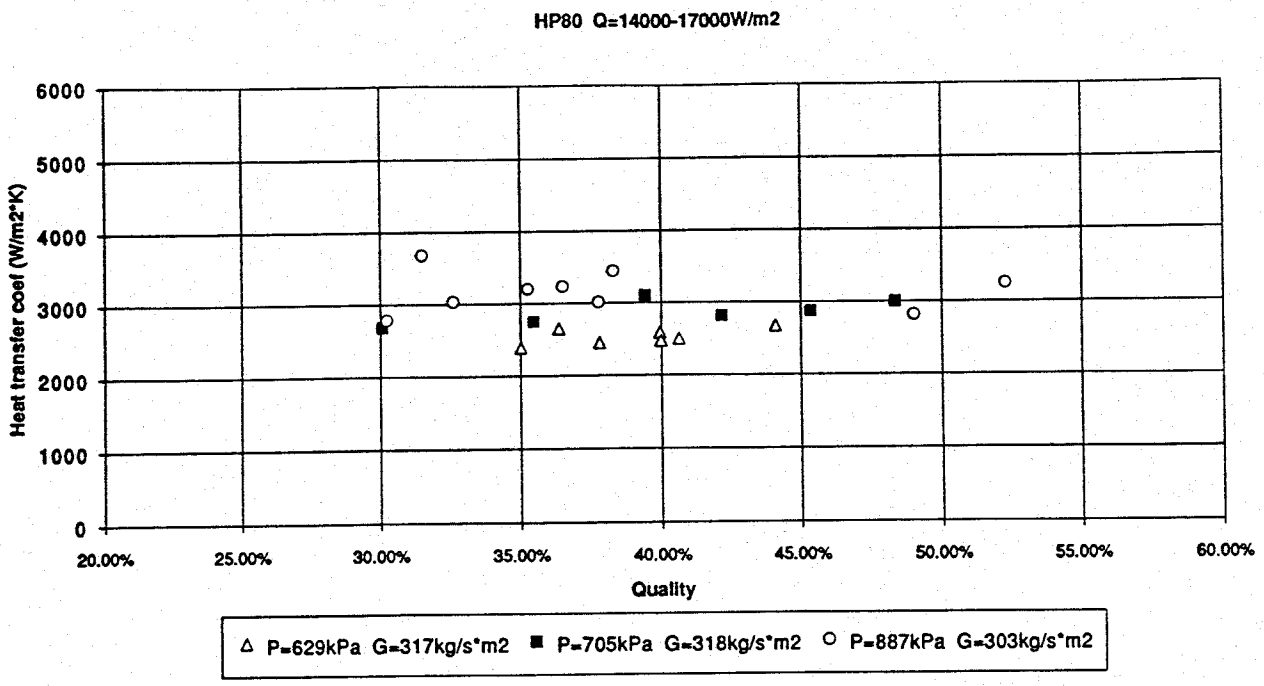

Figure 5(a). HP80 results at three pressures.

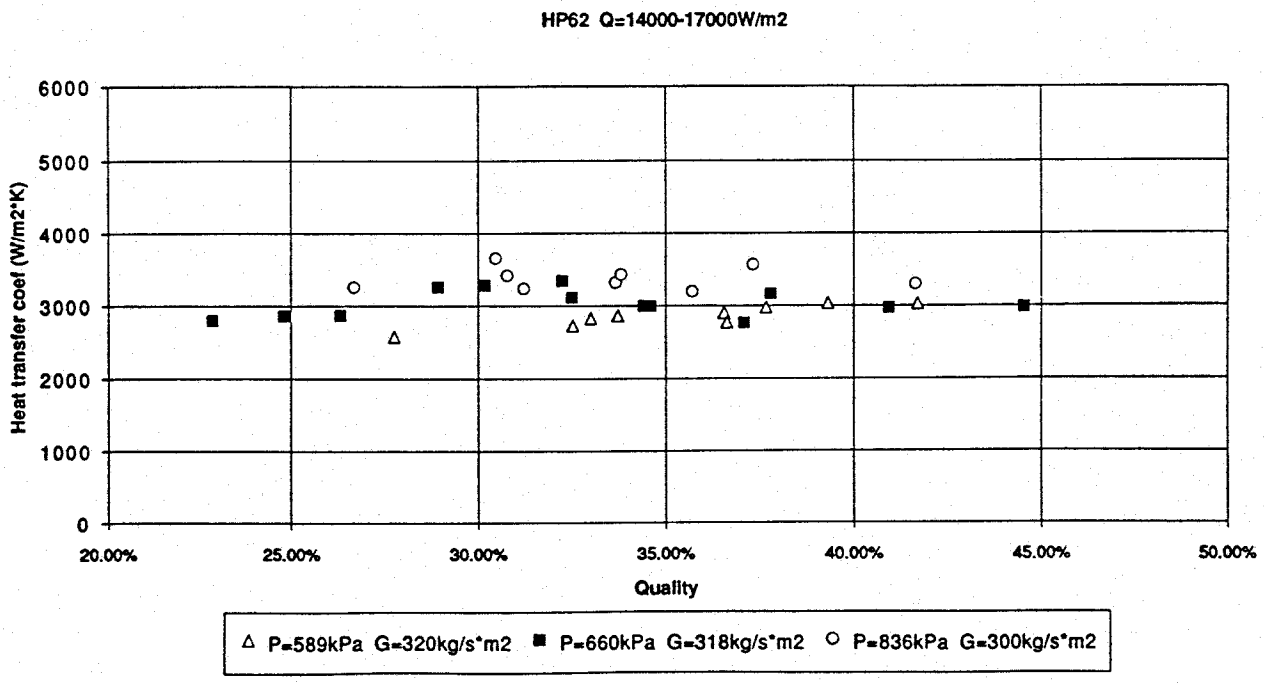

Figure 5(b). HP62 results at three pressures.

Fig. 6(a)

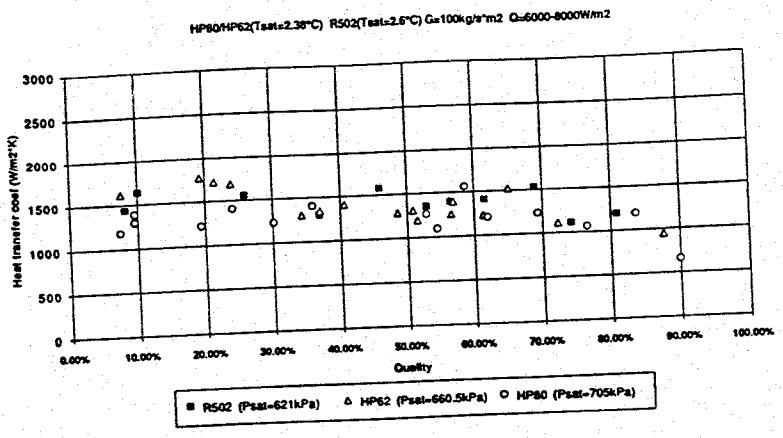

Fig. 6(b)

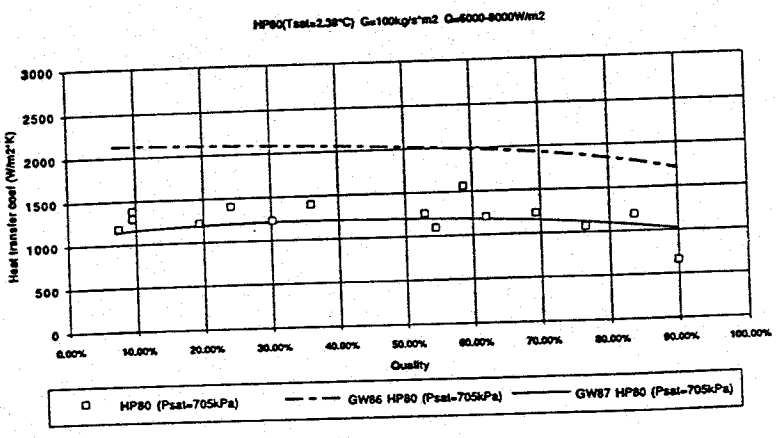

Fig. 6(c)

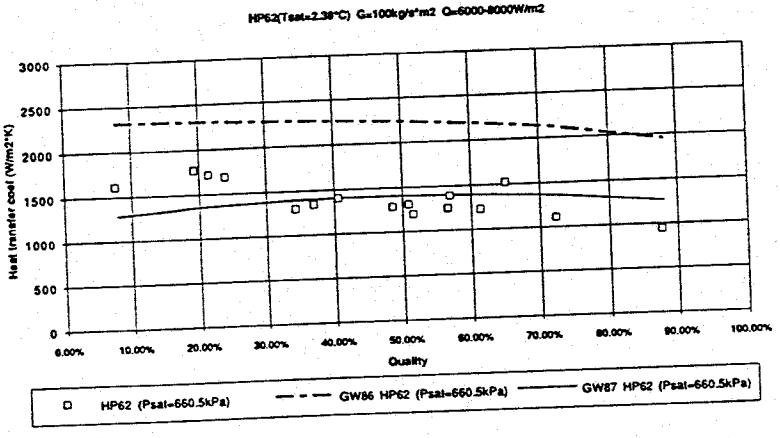

Fig. 6(d)

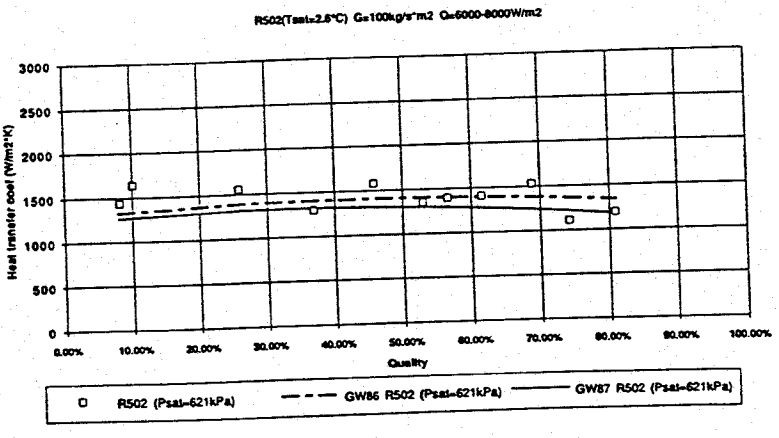

Fig. 7(a)

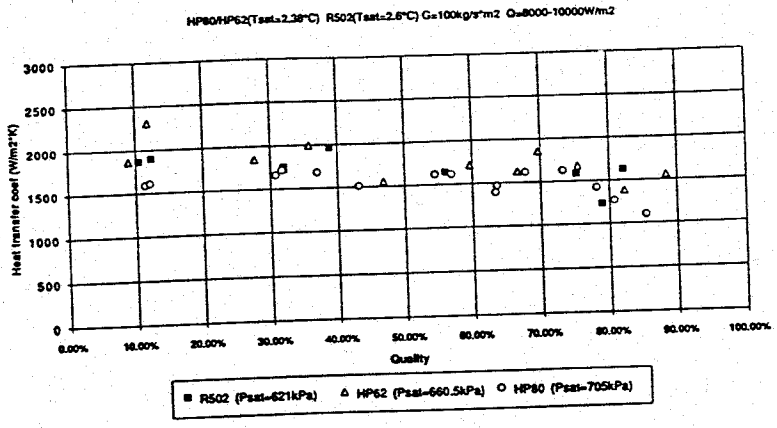

Fig. 7(b)

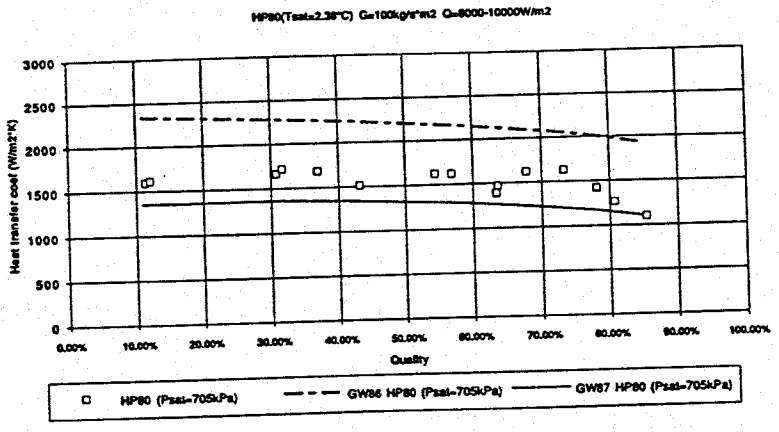

Fig. 7(c)

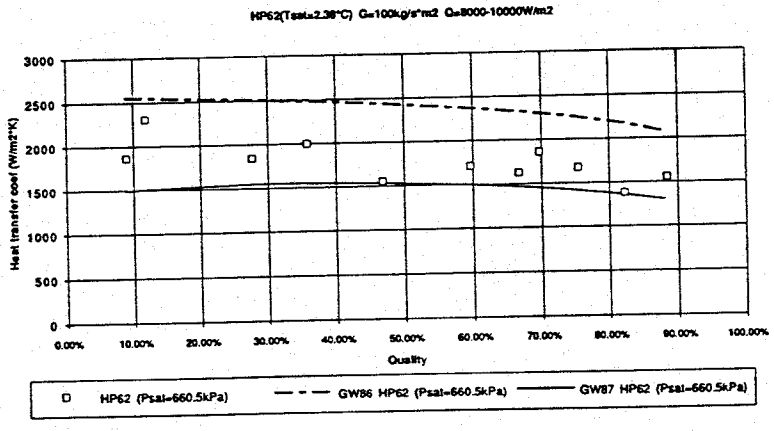

Fig. 7(d)

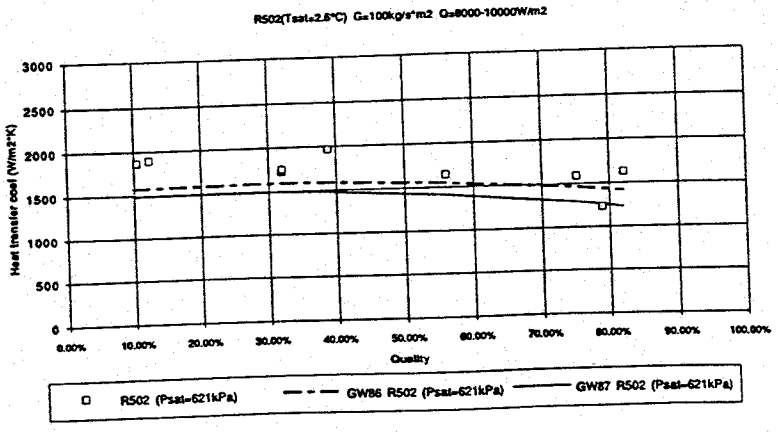

Fig. 8(a)

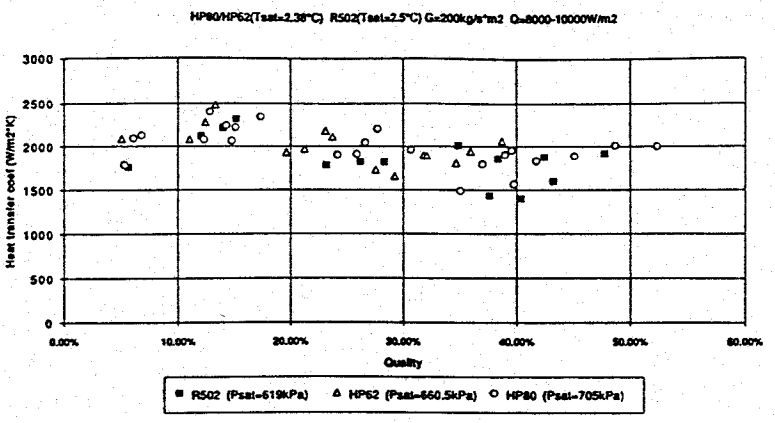

Fig. 8(b)

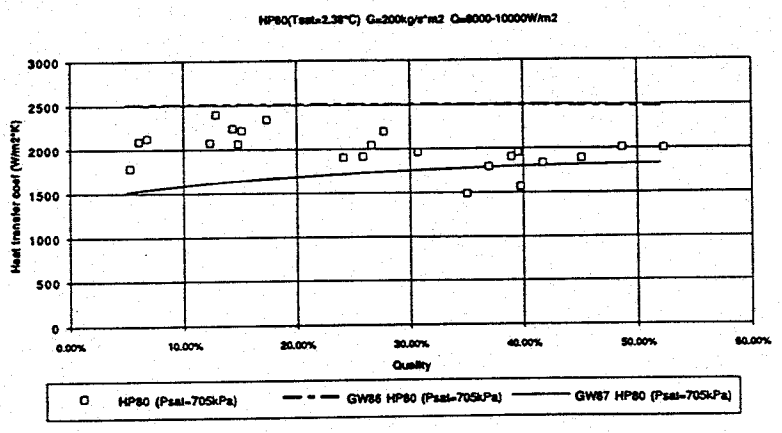

Fig. 8(c)

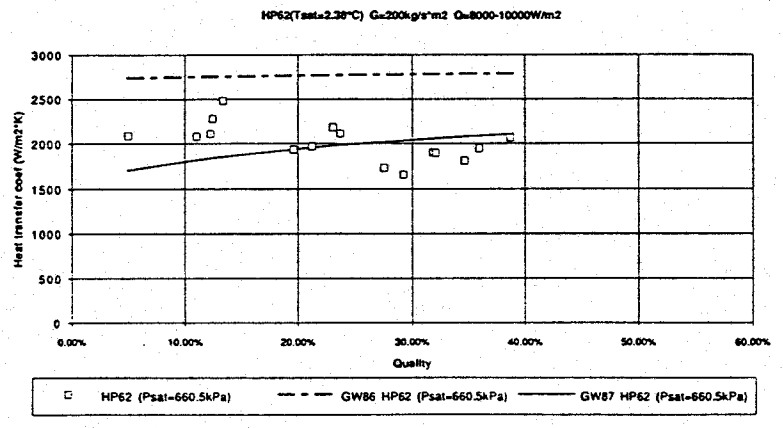

Fig. 8(d)

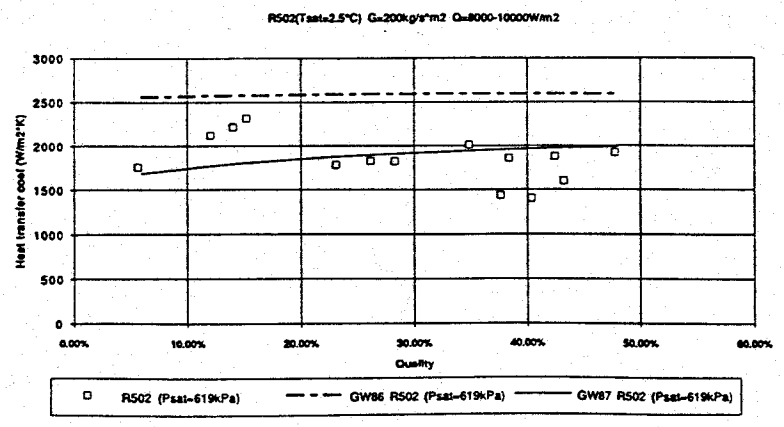

Fig. 9(a)

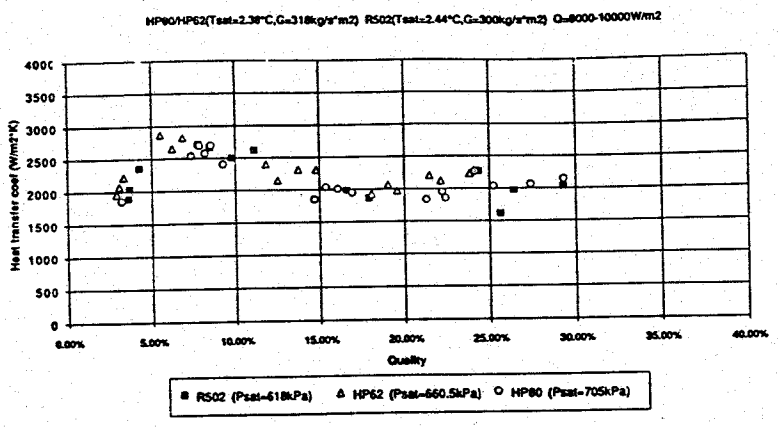

Fig. 9(b)

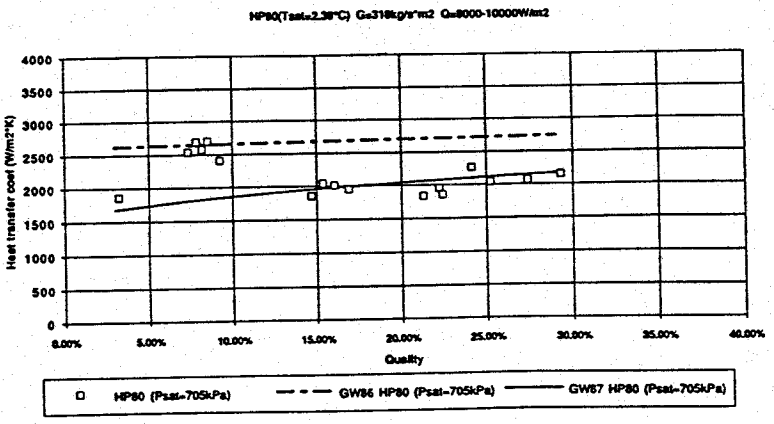

Fig. 9(c)

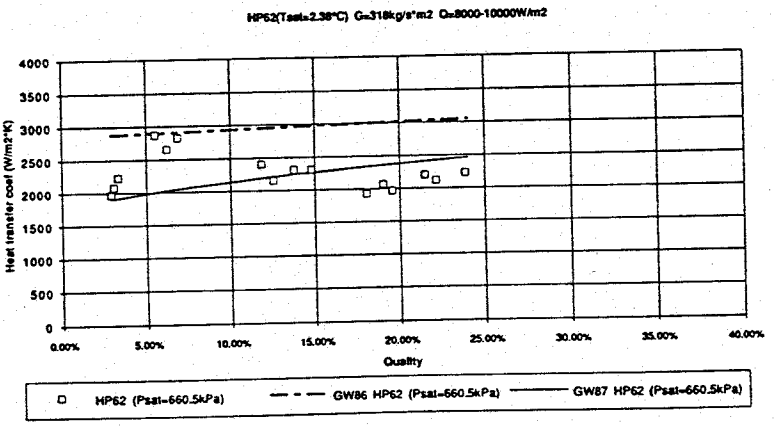

Fig. 9(d)